Learning from Leads: A 1D Dilated ResNet for ECG Chagas Disease Screening

Somesh Saini[1], Matheus Araujo[2]

[1] Computer and Data Sciences, Case Western Reserve University, Cleveland, United States of America
[2] Biomedical Engineering, Case Western Reserve University, Cleveland, United States of America

Abstract

Chagas disease, caused by the parasite Trypanosoma cruzi, presents significant diagnostic challenges due to asymptomatic impacts on heart health and limited resources in the affected areas. We develop a deep-learning model to automate Chagas disease screening using 12-lead electrocardiograms from multiple datasets, including CODE-15, PTB-XL, and SaMi-Trop. We combine automatic hyperparameter optimization and class-imbalance handling with a 1D dilated residual neural network (ResNet) augmented with squeeze-and-excitation (SE) blocks. As part of the George B. Moody PhysioNet Challenge 2025 (Detection of Chagas Disease from the ECG), our team (CLECLINIC) achieved a mean challenge score of 0.198 across the held-out final test set (ranking 24th of 40 teams). Compared with traditional machine-learning baselines, the proposed ResNet delivered a ~4-fold performance gain. These results support the use of deep-learning approaches as a viable tool for scalable, automated Chagas disease screening, particularly in low-resource clinical environments where traditional diagnostics are unavailable.

1. Introduction

Chagas disease, termed *American trypanosomiasis*, is a chronic illness caused by the parasite *Trypanosoma cruzi*, predominantly transmitted through triatomine insects (1). Approximately 8 million people worldwide are infected annually, mainly concentrated in Latin America. Migration patterns have begun to introduce Chagas disease into non-endemic regions, including approximately 300,000 cases in the United States (2). Furthermore, Chagas disease accounts for 670,000 disability-adjusted life-years annually (1). Environmental and socioeconomic factors significantly impact the epidemiology of Chagas disease. Subtropical climates with high humidity, warmer temperatures, and substandard housing conditions proliferate the activity of *Trypanosoma cruzi* parasites and infection (2).

The diagnosis of Chagas disease is a formidable challenge due to the asymptomatic or nonspecific clinical presentation observed in acute and chronic indeterminate phases. Once in the chronic phase, persistent inflammation and damage to myocardial cells can occur in heart tissue with the potential to lead to heart failure.

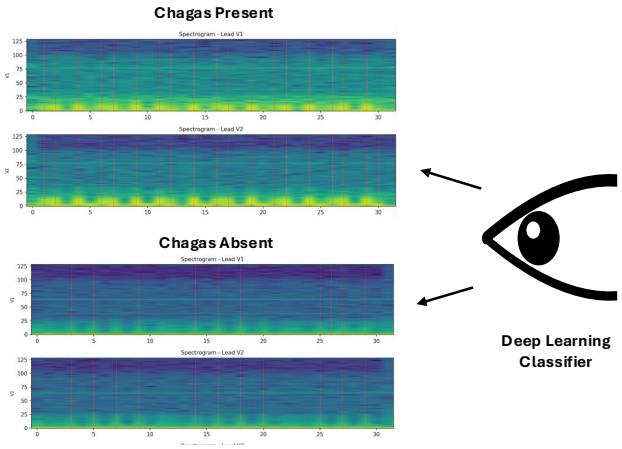

Figure 1: Spectrograms of ECG Data for Leads V1 and V2 with examples from 2 subjects: one with Chagas disease and one without. The brighter colors indicate higher signal energy at the time–frequency, more present in the example with the disease.

Although serological diagnostic methods exist, such as enzyme-linked immunosorbent assays (ELISA) and polymerase chain reaction (PCR) testing, they are resource-intensive, often leading to delayed detection and ineffective disease management for affected patients (2; 3).

Electrocardiograms (ECGs) are crucial for detecting chronic Chagas cardiomyopathy. In Figure 1, we illustrate how visually distinguishable the ECG spectrograms from a Chagas-present and Chagas-absent patients. However, manual ECG interpretation is prone to variability among healthcare providers and is a costly process for interpretation. To address these challenges, the 2025 George B. Moody PhysioNet Challenge aims to advance research by providing large-scale, annotated 12-lead ECG datasets and a standardized framework for developing automated methods for Chagas disease detection (4; 5).

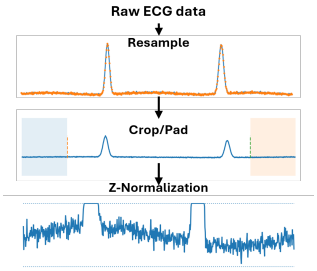

Figure 2: During preprocessing, ECG signals are resampled, cropped/padded, and z-normalized, then passed as input to the model.

In this work, we build on recent advances in Convolutional Neural Networks (CNNs) and residual network (ResNet) variants, which have achieved state-of-the-art performance in ECG classification by extracting complex temporal and spatial features from large datasets(6; 7). Using the 2025 PhysioNet dataset, we apply a ResNet-inspired deep-learning approach for automated Chagas disease detection from 12-lead ECGs. Our objective is to enhance screening availability, improve diagnostic consistency and precision, and ultimately support better patient outcomes.

2. Methodology

The following subsections present the model architecture approach for Chagas classification. Our approach consists of a ResNet Network for prediction. Training utilizes an imbalance-aware strategy and precision-recall curve calibration.

For comparison purposes, we experimented with alternative machine learning methods, including a Random Forest model combined with features extracted via `tsfresh`.

2.1. Data

This study uses three datasets from the PhysioNet 2025 Challenge for model training, each offering different demographic, geographic, and clinical characteristics relevant to the detection of Chagas disease (8). The CODE-15 dataset comprises 345,779 ECG recordings from 233,770 patients, collected through the Minas Gerais Telehealth Network in Brazil. These recordings include self-reported cases of Chagas disease and are available in 7.3-second or 10.2-second durations, sampled at 400 Hz. 1.91% of the records were labeled as Chagas-positive and 98.09% as Chagas-negative (9). The PTB-XL dataset provides 21,799 ECG records from 18,869 European patients, each 10.0 seconds in length and sampled at 500 Hz. It contains only Chagas-negative cases, making it valuable for training balanced models and generalization (10). Finally, the SaMi-Trop dataset contains 1,631 ECGs from 1959 patients, specifically validated for chronic Chagas cardiomyopathy, where all cases are Chagas-positive. Specifically, it includes women aged 50 to 74 years of age from lower socioeconomic backgrounds, with recordings of 7.3 or 10.2-second durations and a sampling frequency of 400 Hz, offering high clinical relevance for Chagas-specific modeling (11). Note that the validation and test data are comprised of multiple datasets with strong labels; these datasets are distinct from the training set.

2.2. Preprocessing

All raw 12-lead ECGs were standardized with a three-stage preprocessing pipeline as shown in Figure 2. First, signals were resampled to 500 Hz so that recordings from different sources shared the same frequency content. Second, to present a uniform input size, each record was converted to a fixed 5120-length window. Traces shorter than the set length were zero-padded, and longer traces were centered and trimmed accordingly. Third, we normalized each lead by median-centering and median absolute deviation (MAD) scaling, removing offset and placing amplitudes on a common scale, robust to ECG outliers.

For lead ℓ with samples $x_\ell(t)$,

$$z_\ell(t) = \mathrm{clip}_{[-5,5]}\left(\frac{\mathrm{x}_\ell(\mathrm{t}) - \mathrm{median}(\mathrm{x}_\ell)}{\mathrm{MAD}(\mathrm{x}_\ell) + 10^{-6}}\right)$$

$$\mathrm{MAD}(x) = \mathrm{median}\big(|x - \mathrm{median}(x)|\big)$$

The first equation highlights the z-normalization process applied to all ECG signals. The $\mathrm{clip}_{[-5,5]}$ interval is applied on the z-score, capping standardized values at ± 5 to suppress extreme outliers. The second equation defines the median absolute deviation (MAD), which measures variability by taking the median of absolute deviations from the median.

2.3. Model Architecture

We use a compact dilated residual 1-dimensional (1D) ResNet CNN with squeeze-and-excitation (SE) and Group Normalization (12; 13). The network processes the preprocessed 12-lead ECG segment through three residual convolutional blocks as shown in Figure 3. Each block contains a 1D convolution (*Conv1d*) with a 3x1 kernel and increasing dilation rates (1, 2, and 4), enabling the model to capture progressively wider temporal contexts within the receptive field while preserving signal resolution. This is followed by a GroupNorm layer to rescale ECG feature maps across leads, and ReLU activation. When moving to the next residual block, we use a 1x1 *Conv1d*. The ECG sequence length is gradually reduced between blocks via max pooling.

While training, data was processed as tensors below (Length, Channels):

$$(5120, 12) \xrightarrow[\text{Block 1 } (d=1)]{\text{MaxPool}} (2560, 64) \xrightarrow[\text{Block 2 } (d=2)]{\text{MaxPool}} (1280, 128) \xrightarrow[\text{Block 3 } (d=4)]{\text{GlobalMaxPool}} (1, 256)$$

Ultimately, the classifier head operates on the pooled

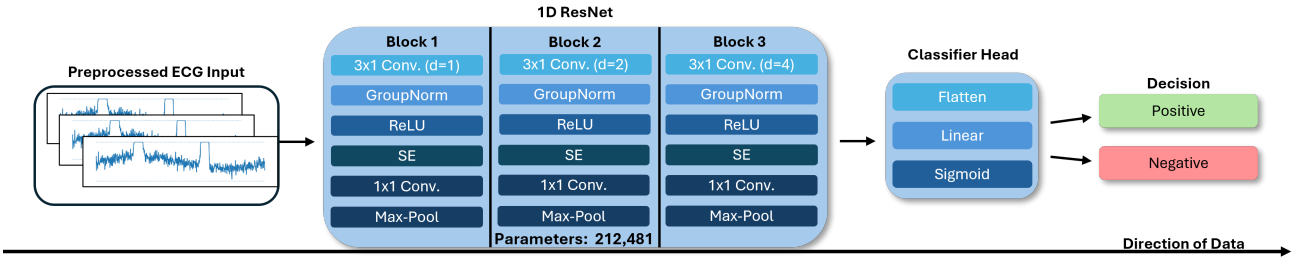

Figure 3: Model architecture with data flowing from left (raw data) to right (classification labels). The 1D ResNet processes each ECG segment through three residual blocks with increasing dilation (1–4) to expand the receptive field. The flattened features feed a linear layer with sigmoid to produce a classification probability.

features by flattening them into a single vector and passing them through a fully connected neural network with a sigmoid activation to output the probability of Chagas disease. The model was implemented in Python 3.13.0 using PyTorch 2.1.2.

2.4. Training and Inference

We trained the model using stratified $90/5/5$ respective train, validation, and test splits. To improve robustness, we applied data augmentations including Gaussian noise, scale jitter, and mixup. Training employed Focal Loss ($\alpha = 0.5$, $\gamma = 1.5$), which emphasizes rare positive cases and mitigates the effects of the 1:30 positive–negative class imbalance. We optimized the 1D ResNet model with *AdamW* under a *OneCycleLR* schedule. The OneCycleLR schedule helped the optimizer explore a wide learning-rate range and converge more efficiently. For stability on ECG sequences, we enable exponential moving average (EMA) of weights to reduce variance and yield better generalization. The final training uses early stopping (patience$= 4$) to limit overfitting.

In Table 1, we show the selected hyperparameters with Optuna (30 trials) over augmentation metrics (noise, scale jitter, mixup), optimizer settings (learning rate, weight decay), and model depth (number of residual blocks). After training, we pick a single final decision threshold on the validation split by maximizing F_1 on the precision–recall curve, and we use this fixed threshold at inference to convert probabilities into class labels.

2.5. Evaluation

For consistency with the PhysioNet Challenge framework, we submitted all trained models to the official challenge organizers. The submitted model performance was evaluated on a hidden validation and test set and returned the Challenge Score, which served as the primary criterion for ranking models (4). Since the Challenge setting included multiple competitors and limited each team to only ten submission attempts, careful model selection and tuning were necessary. While additional internal metrics (AUROC, AUPRC, F1) were monitored during development,

Hyperparameter	Value / Description
Sequence length	5120
Number of residual blocks	3
Base channel width	64
Dropout rate	0.26
Mixup coefficient	0.04
Noise sigma	0.02
Input scaling range	[0.99, 1.01]
Stochastic drop probability	0.06
Classification threshold	0.53
Softmax temperature	0.58
EMA decay rate	0.99

Table 1: Final hyperparameter configuration for the 1D ResNet model, obtained via Optuna optimization in the local experimental environment.

the Challenge Score ultimately determined our comparative evaluation.

3. Results

In Table 3, we present our results during the validation phase. The best performance was obtained with a 1D ResNet model, receiving a validation score of 0.271, an AUROC of 0.70, and an accuracy of 0.98. While comparing multiple models, including machine learning classifiers with tsfresh-based feature extraction, we observed that traditional approaches reached substantially lower challenge scores (e.g., Random Forest-based models reached 0.097 and 0.062) with close to random AUROC performance.

The official evaluation was performed in a separate hidden test set based on the model of the validation phase. Our approach achieved a mean score of 0.198, ranking 24th out of 40 in the CinC competition. Our final submission on the test set is summarized in Table 2.

Model ID	Mean Score	REDS-II	SaMi-Trop III	ELSA-Brasil
2684	0.198	0.246	0.277	0.071

Table 2: Overall final scores in PhysioNet challenge test datasets, including per-dataset performance.

Model (ID)	Architecture	HPO	Score	AUROC	AUPRC	Accuracy	F1
Model 9 (2684)	ResidualDilatedBlocks + SE	Optuna	0.271	0.701	0.122	0.980	0.013
Model 7 (2627)	ResidualDilatedBlocks + SE	Optuna	0.270	0.671	0.119	0.980	0.020
Model 8 (2617)	No Residual 3-Block CNN	Optuna	0.262	N/A	N/A	N/A	N/A
Model 6 (2564)	ResidualDilatedBlocks	Optuna	0.236	0.677	0.094	0.977	0.098
Model 1 (2061)	ResidualDilatedBlocks + SE	Optuna	0.230	0.653	0.058	0.971	0.076
Model 5 (2560)	ResidualDilatedBlocks	Optuna	0.215	0.667	0.073	0.979	0.038
Model 2 (2443)	Dilated Conv. Blocks	Optuna	0.194	0.612	0.061	0.978	0.094
Model 3 (2342)	RandomForestClassifier + tsfresh	GridSearchCV	0.097	0.526	0.025	0.979	0.000
Model 4 (2494)	ResidualDilatedBlocks + SE	Optuna	0.050	0.500	0.021	0.979	0.000
Baseline Model	RandomForestClassifier	N/A	0.062	N/A	N/A	N/A	N/A

Table 3: PhysioNet Official validation phase: Model comparison across architectures and hyperparameter optimization (HPO).

4. Discussion

Our results suggest that a dilated 1D SE ResNet can learn and discriminate features from 12-lead ECG data for automated Chagas screening. We also demonstrated that deep learning architectures are more capable of capturing complex temporal dependencies in ECG signals compared to traditional machine learning models, such as Random Forest.

We noticed two main challenges during this project. First, the 90/5/5 validation data split and its impact on heavy calibration efforts. With the 1:30 class imbalance, very few positive cases were in the 5% validation split, which introduces statistical uncertainty in the precision–recall curve and calibration performance. We also explored Synthetic Minority Oversampling (SMOTE) to mitigate the 1:30 class imbalance, but applying it to thousands of 12-lead ECG sequences was prevented by memory limits. As a result, we adopted a lightweight sampling strategy with focal loss. This function down-weights easy negatives and gives more weight to the rare positive cases, providing a reasonable improvement for model learning despite the imbalance. Future work, with robust computing resources, could revisit imbalance handling in stratified split adjustments and synthetic oversampling.

5. Conclusion

We demonstrate that a dilated 1D ResNet achieves approximately 4-fold gains over traditional machine learning baselines. We emphasize that learning discriminative features for Chagas disease from 12-lead ECGs is possible. This approach achieved competitive results in the PhysioNet 2025 Challenge under the constraint of limited submissions. Our findings highlight the potential for scalable Chagas disease screening in resource-constrained areas.

References

[1] Moncayo and A. C. Silveira, "Current Epidemiological Trends for Chagas Disease in Latin America and Future Challenges in Epidemiology, Surveillance and Health Policy," *Memórias do Instituto Oswaldo Cruz*, vol. 104, no. Suppl 1, pp. 17–30, 2009.

[2] C. Bern and S. P. Montgomery, *Chagas Disease (American Trypanosomiasis)*, 10th ed. Elsevier, 2020. [Online]. Available: https://www.ncbi.nlm.nih.gov/books/NBK459272/

[3] J. C. P. Dias, "Elimination of Chagas Disease Transmission: Perspectives," *Memórias do Instituto Oswaldo Cruz*, vol. 104, no. Suppl 1, pp. 41–45, 2009.

[4] M. A. Reyna, Z. Koscova, J. Pavlus, J. Weigle, S. Saghafi, P. Gomes, A. Elola, M. S. Hassannia, K. Campbell, A. Bahrami Rad, A. H. Ribeiro, A. L. P. Ribeiro, R. Sameni, and G. D. Clifford, "Detection of Chagas Disease From the ECG: The George B. Moody PhysioNet Challenge 2025," *Computing in Cardiology*, vol. 52, pp. 1–4, 2025.

[5] M. A. Reyna, Z. Koscova, J. Pavlus, S. Saghafi, J. Weigle, A. Elola, S. Seyedi, K. Campbell, Q. Li, A. Bahrami Rad, A. Ribeiro, A. L. P. Ribeiro, R. Sameni, and G. D. Clifford, "Detection of Chagas Disease From the ECG: The George B. Moody PhysioNet Challenge 2025," arXiv preprint, 2025, arXiv:2510.02202. [Online]. Available: https://arxiv.org/abs/2510.02202

[6] A. Saglietto, D. Baccega, R. Esposito, M. Anselmino, V. Dusi, A. Fiandrotti, and G. M. De Ferrari, "Convolutional Neural Network (CNN)-Enabled Electrocardiogram (ECG) Analysis: A Comparison Between Standard Twelve-Lead and Single-Lead Setups," *Frontiers in Cardiovascular Medicine*, vol. 11, p. 1327179, 2024.

[7] J. Li, S.-p. Pang, F. Xu, P. Ji, S. Zhou, and M. Shu, "Two-Dimensional ECG-Based Cardiac Arrhythmia Classification Using DSE-ResNet," *Scientific Reports*, vol. 12, no. 1, p. 14485, 2022.

[8] A. L. Goldberger, L. A. N. Amaral, L. Glass, J. M. Hausdorff, P. C. Ivanov, R. G. Mark, J. E. Mietus, G. B. Moody, C.-K. Peng, and H. E. Stanley, "PhysioBank, PhysioToolkit, and PhysioNet: Components of a New Research Resource for Complex Physiologic Signals," *Circulation*, vol. 101, no. 23, pp. e215–e220, 2000.

[9] A. H. Ribeiro, G. M. Paixao, E. M. Lima, M. Horta Ribeiro, M. M. Pinto Filho, P. R. Gomes, D. M. Oliveira, W. Meira Jr., T. B. Schön, and A. L. P. Ribeiro, "CODE-15%: A Large-Scale Annotated Dataset of 12-Lead ECGs," 2021. [Online]. Available: https://zenodo.org/records/4916206

[10] P. Wagner, N. Strodthoff, R.-D. Bousseljot, W. Samek, and T. Schaeffter, "PTB-XL: A Large Publicly Available Electrocardiography Dataset (Version 1.0.3)," 2022. [Online]. Available: https://physionet.org/content/ptb-xl/1.0.3/

[11] A. L. P. Ribeiro, A. H. Ribeiro, G. M. Paixao, E. M. Lima, M. Horta Ribeiro, M. M. Pinto Filho, P. R. Gomes, D. M. Oliveira, W. Meira Jr., T. B. Schön, and E. C. Sabino, "SaMi-Trop: 12-Lead ECG Traces With Age and Mortality Annotations," 2021. [Online]. Available: https://zenodo.org/records/4905618

[12] K. He, X. Zhang, S. Ren, and J. Sun, "Deep Residual Learning for Image Recognition," in *Proceedings of the IEEE Conference on Computer Vision and Pattern Recognition*, 2016, pp. 770–778.

[13] Y. Wu and K. He, "Group Normalization," in *Proceedings of the European Conference on Computer Vision (ECCV)*, 2018, pp. 3–19.

Address for correspondence:

Somesh Saini

3919 Magnolia Circle Maumee, Ohio, 43537

sbs166@case.edu